Rev. Mexicana Astron. Astrof., 17, 65-74 (1989)

ON THE STRUCTURE OF STEADY STELLAR JETS: AN ANALYTIC MODEL

J. Cantó

Instituto de Astronomía
Universidad Nacional Autónoma de México

and

A.C. Raga and L. Binette

Canadian Institute for Theoretical Astrophysics, Canada

Received 1989 April 20

RESUMEN

Se presentan resultados analíticos sobre la estructura interna de chorros estelares estacionarios como complemento a estudios numéricos. Se hace especial énfasis en las propiedades (forma, separación, etc.) de los choques internos en los chorros. El modelo es aplicable a chorros delgados y altamente supersónicos con presión inical mayor a la del medio ambiente, que se mueven en un medio uniforme. Se presentan expresiones analíticas sencillas para los principales parámetros del flujo, tales como la distancia entre choques y la velocidad de choque. Se encuentra que la forma del choque incidente es un arco de circunferencia que pasa por el punto de inyección. También, se muestra que la velocidad de choque es *siempre* $\sim$ 20 km s^{-1} para choques radiativos con temperatura de equilibrio $\sim 10^4$ °K. Este resultado es independiente de los parámetros del chorro o los del medio ambiente.

ABSTRACT

We present the results of an analytic study of the internal structure of steady stellar jets as a complement to previous numerical investigations. Special emphasis is made on the properties (shape, separation, etc.) of the crossing-shocks within the jet. The model is restricted to initially underexpanded, highly supersonic narrow jets moving into a uniform medium. Simple analytic expressions are given for the main parameters of the flow, such as the distance between crossing-shocks and the shock velocity. It is found that the shape of the incident shock is an arc of circumference passing through the injection point. Also, we show that the shock velocity is *always* $\sim$ 20 km s^{-1} for radiative shocks with equilibrium temperature of $\sim 10^4$ °K, a result which is independent of the parameters of the jet as well as those of the ambient medium.

Key words: HYDRODYNAMICS – INTERSTELLAR MEDIUM – SHOCK WAVES

I. INTRODUCTION

During the last few years, deep images in the vicinity of young low-mass stars and Herbig-Haro objects have revealed the presence of faint, line-emitting filamentary structures closely related to them. These structures are particularly evident in the Hα and [S II] lines.

Up to now, more than twenty young stellar objects have been reported to have such associated line-emitting filaments. The main observational characteristics of these structures are compiled and discussed in a series of recent review papers by Mundt (see for instance Mundt 1988 and references therein). Among their observational properties we may distinguish: 1) projected length in the range 0.02 – 0.5 pc; 2) length-to-width ratio $\sim$ 10 –20; 3) electron densities $\sim$ 500 – 2000 cm^{-3}; 4) emission-line spectrum similar to that of H-H objects, indicative of shock-excitation with low shock velocities $\sim$ 20 – 100 km s^{-1}; 5) radial velocity of the emitting material with respect to the parent cloud of up to 400 km s^{-1}, with typical values in the range 50 – 100 km s^{-1}.

In some cases (for instance R Mon, RCrA, HH57, HL Tau and XZ Tau), these filamentary structures could simply be the light emitted by, or reflected from, the walls of cavities created by the sweeping action of strong stellar winds (Cantó, Sarmiento and Rodríguez 1986). When viewed from certain positions the radiation from these walls appears to the observer as elongated structures.

However, most authors interpret them as jets of supersonic material, collimated in the immediate vicinity of stars, and ramming into the molecular cloud. Their characteristic emission line spectrum and the knotty morphology observed in some of them (in particular in HH34–IRS; Reipurth *et al.* 1986, Mundt 1986; Raga and Mateo 1988; Bührke, Mundt and Ray 1988) are explained in terms of internal shocks along the jet, similar to those seen in laboratory experiments.

The flow pattern produced by a supersonic jet running into the interstellar medium can be divided into three basic regions (Blandford and Rees 1974): the jet itself; the working surface (that is, the region where the jet collides with the ambient medium); and the cocoon, which engulfs the jet and is formed by the backward movement of the shocked jet material.

The structure of the working surface is unsteady and very complex; thus, it can only be studied in detail through numerical simulations such as those performed by Norman *et al.* (1982), Tenorio-Tagle, Rozyczka and Cantó (1986), Tenorio-Tagle and Rozyczka (1988), Raga (1989), and Blondin, Königl and Fryxell (1989). The main body of the jet, on the other hand, can be regarded as steady except near the working surface (Falle, Innes and Wilson 1987; Tenorio-Tagle and Rozyczka 1988). This, of course, provided that the boundary of the jet is not subject to pressure and cross-section perturbations due, for instance, to Kelvin-Helmholtz instabilities. The effects of such instabilities on the structure of the jet have been the subject of several studies (e.g., Norman *et al.* 1982; Cohn 1983; Payne and Cohn 1985; Ferrari, Trussoni and Zaninetti 1981; Silvestro *et al.* 1987), although laboratory experiments indicate that K–H instabilities are not excited for high enough ($\geq$ 4000) Reynold's numbers (Crighton 1981).

The structure of the steady part of the jet in the presence of a non-uniform external medium has been studied in a series of very stimulating papers by Sanders (1983), Falle and Wilson (1985), Wilson and Falle (1985), Wilson (1987*a,b*), and Falle *et al.* (1987). They find (as first predicted by Prandtl 1907) that the jet develops a chain of steady crossing-shock patterns of internal shock waves associated with variations in its width. The distance between two consecutive crossing-shocks is roughly the Mach number of the jet times its width. Each of these patterns consists of an incident conical shock which starts to develop near the boundary of the jet and propagates inwards to the axis; and a reflected shock which runs from the axis to the boundary. An important property of the incident shocks is that they recollimate the jet since the flow is turned towards the axis upon passing through these shocks. This reconfining mechanism allows the jet to travel long distances until it is destroyed by the turbulent boundary layer, becoming wholly subsonic and mixing with the interstellar medium.

So far, the studies of the detailed structure of these crossing-shocks within steady jets have been performed by the direct numerical integration of the gas dynamics equations. Although this procedure has the benefit of allowing the study of the phenomenon without making any gross approximation, it has the limitation that it is sometimes rather difficult to reach general conclusions or to extend the results to conditions other than those assumed in the calculations.

In this paper we present the results of an analytic study of the internal structure of steady jets, as a complement to previous numerical works. Special emphasis is made on the properties (shape, separation, etc.) of the crossing-shocks. In order to make the problem solvable by analytic methods, we will restrict ourselves to initially underexpanded (jet pressure greater than ambient pressure) and highly supersonic narrow jets moving into a uniform medium. In this case, the internal crossing-shocks are produced as the jet tries to match its pressure with that of the ambient medium.

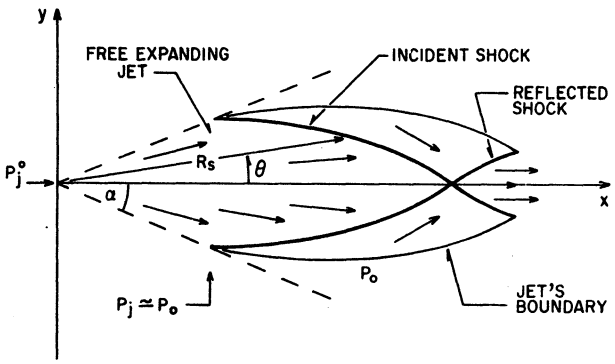

Fig. 1. Sketch of the first crossing-shock within an underexpanded jet. Initially the jet expands freely with an opening angle α until its pressure falls below the pressure P_0 of the ambient medium. Beyond this point the jet becomes reconfined by an incident conical shock. The flow is then turned along the axis through a reflected conical shock.

II. THE MODEL

a) *Basic Equations*

Consider the steady part of a highly underexpanded and highly supersonic jet moving into a uniform medium. Let V_j°, P_j° and c_j° be the initial velocity, pressure and (adiabatic) sound speed of the jet; and P_0 the pressure of the surrounding medium. The jet has cylindrical symmetry; let x and y be the distances along and perpendicular to the axis of the jet respectively. The origin is the injection point (see Figure 1).

As the underexpanded jet comes out into the lower pressure medium, it first undergoes a Prandtl-Meyer expansion to decrease its pressure. The jet boundary expands and a rarefaction wave propagates through the body of the jet towards the symmetry axis. The outer layer of the jet expands laterally with a constant maximum velocity given by

$$U_m = \frac{2(1-\kappa)}{(\gamma-1)} c_j^\circ \quad , \tag{1}$$

with γ the (constant) ratio of specific heats, and

$$\kappa \equiv \left(\frac{P_0}{P_j^\circ}\right)^{(\gamma-1)/2\gamma} \quad . \tag{2}$$

The sudden lateral expansion of the jet causes a rapid decrease in pressure in the flow. Once the pressure gradients become negligible, there is an absence of forces acting on the flow, and there will be no redistribution of mass. Hence the density profile will remain self-similar, scaling simply as $1/R^2$; where R is the distance to the injection point. The density distribution is thus determined near the origin of the jet, where pressure forces are important, and remains frozen beyond this point. Thus, the density distribution depends on the injection conditions and can only be found by solving the complete gas dynamic equations. It is impossible to find an exact analytic solution to the problem for arbitrary (and highly uncertain) initial conditions. In view of this limitation, we adopt the simplest assumption, i.e., that the density distributions is only a function of R, and is of the form

$$\rho_j(R) = \frac{A}{R^2} \quad , \tag{3}$$

where A is a constant. In order to relate A to the initial conditions of the jet, we will adopt the following approximations. First, we will assume that the jet retains its bulk velocity, despite the downstream accelaration resulting from its rapid decrease in pressure. This assumption is valid for highly supersonic jets. Second, we will assume that the jet expands laterally at an opening angle α (see Figure 1) given by

$$\sin\alpha = \frac{U_m}{V_j} = \frac{2(1-\kappa)}{(\gamma-1)}\frac{1}{M_j^\circ} \quad , \tag{4}$$

where M_j° is the jet's Mach number at injection.

Assuming further that the velocity vector is directed radially away from the injection point, equation (3) can be rewritten as

$$\rho_j(R) = \frac{\dot{M}_j}{2\pi V_j^\circ(1-\cos\alpha)R^2} \quad , \tag{5}$$

where $\dot{M}_j$ is the mass loss rate in the jet.

As mentioned above, the pressure decreases very rapidly along the jet (see the Appendix)

$$P_j \sim \rho_j^\gamma \sim R^{-2\gamma} = R^{-10/3}, \gamma = 5/3 \quad , \tag{6}$$

for an adiabatic expansion. Therefore, the internal pressure of the free expanding jet will eventually fall below the pressure P_0 of the ambient medium. At this point, the jet will become reconfined by the stronger external pressure. Since the Mach number of the jet increases with distance from the injection point

$$M_j \sim \rho_j^{-(\gamma-1)/2} \sim R^{(\gamma-1)} = R^{2/3}, \gamma = 5/3 \quad ; \tag{7}$$

the reconfinement generates an internal shock (the incident shock in the standard nomenclature; see Figure 1). Behind this shock the pressure of the shocked flow nearly matches the pressure of the ambient medium and the shock remains steady at a fixed position (see equations (8) and (9)). The flow continuously passing through the shock is turned towards the axis.

The locus of this shock (strictly speaking, the locus of the intersection of this shock, which is a surface, with a plane containing the symmetry axis) can be found from the condition of pressure balance

$$\epsilon_I \rho_j V_{jn}^2 + P_{CE} = P_0 \quad , \tag{8}$$

where ϵ_I is a parameter of order unity ($= 2/(\gamma+1)$ if the shock is adiabatic; $\cong 1$ if the shock is radiative), V_{jn} is the component of the velocity of the jet normal to the shock, and P_{CE} is the centrifugal pressure exerted by the shocked flow (see Cantó 1980 for details concerning this pressure). Equation (8) assumes the shock to be strong.

Since we are interested in highly supersonic jets, the angle α (see equation (4)) is expected to be small and the shock to be rather elongated. Thus, the shocked material will move nearly parallel to the axis of the jet. In this case, the centrifugal pressure is also expected to be small (compared with the other terms in equation (8)). Neglecting the centrifugal pressure, equation (8) reduces to

$$\epsilon_I \rho_j V_{jn}^2 \cong P_0 \quad . \tag{9}$$

Let $R_S(\theta)$ be the locus of the incident shock; where θ is the angle to the symmetry axis measured counterclockwise from the axis (see Figure 1). Then,

$$V_{jn} = V_j^\circ \frac{R_S}{(R_S^2 + R_S'^2)^{1/2}} \quad , \tag{10}$$

where $R'_S \equiv dR_S/d\theta$. Substitution of equations (5) and (10) in equation (9) yields

$$P_0 = \frac{\epsilon_I \dot{M}_j V_j^\circ}{2\pi(1-\cos\alpha)}\frac{1}{(R_S^2 + R_S'^2)} \quad . \tag{11}$$

Defining

$$R_0 \equiv \left[\epsilon_I \dot{M}_j V_j^\circ / 2\pi(1-\cos\alpha)P_0\right]^{1/2} \quad , \tag{12}$$

and

$$r \equiv R_S/R_0 \quad , \tag{13}$$

equation (11) can be written as

$$r^2 + r'^2 = 1 \quad , \tag{14}$$

where $r' \equiv dr/d\theta$. Equation (14) admits the general solution

$$r = \sin(\phi \pm \theta) \quad , \tag{15}$$

where ϕ is a constant. This solution represents two circumferences (one for each sign) of radius 1/2 and passing through the origin. One of them (the plus sign) is centered at: $x_0 = 1/2 \sin\phi$, $y_0 = 1/2 \cos\phi$ while the other (the minus sign) is centered at: $x_0 = 1/2 \sin\phi$, $y_0 = -1/2 \cos\phi$. The locus of the shock is given by the arc with $y > 0$ of the minus sign solution and the arc with $y < 0$ of the plus sign solution.

The constant ϕ, which determines the solution, can be estimated by demanding that the pressure in the jet equals the outside pressure at the intersection between the shock (equation 15) and the boundary of the jet ($\theta = \alpha$). That is, we require that the shock starts at the boundary of the jet. This is done in the Appendix and the result is

$$\phi = \alpha + \arcsin\left[\frac{1}{(\gamma\epsilon_I)^{1/2}} \frac{\kappa}{M_j^\circ}\right] \quad . \tag{16}$$

We note that the dependence of ϕ on the pressure ratio P_0/P_j° (see equation (4)) is rather weak since $(\gamma - 1)/2\gamma = 0.2$ for $\gamma = 5/3$.

For a hypersonic jet ($M_j^\circ \gg 1$)

$$\phi \cong \alpha\left[1 + \frac{(\gamma - 1)}{2} \frac{1}{(\gamma\epsilon_I)^{1/2}} \frac{\kappa}{(1 - \kappa)}\right] \quad ; \tag{17}$$

where we have used equation (4).

It is easy to see from equation (15) that the shock intersects the axis of the jet at a distance (in units of R_0) from the injection point

$$a = \sin\phi \quad , \tag{18}$$

and that the maximum distance (also in units of R_0) between the shock and the axis is,

$$b = \frac{1}{2}(1 - \cos\phi) \quad . \tag{19}$$

The distance

$$aR_0 = \sin\phi\left[\frac{\epsilon_I \dot{M}_j V_j^\circ}{2\pi(1 - \cos\alpha)P_0}\right]^{1/2} \quad , \tag{20}$$

with ϕ given by equation (16), thus represents the position of the center of the first crossing-shock; while

$$2bR_0 = (1 - \cos\phi)\left[\frac{\epsilon_I \dot{M}_j V_j^\circ}{2\pi(1 - \cos\alpha)P_0}\right]^{1/2} \tag{21}$$

gives the maximum width of the shock.

For a highly supersonic jet, equations (20) and (21) reduce to

$$aR_0 \simeq \frac{\phi}{\alpha}\epsilon_I^{1/2}\left(\frac{\dot{M}_j V_j^\circ}{\pi P_0}\right)^{1/2} \simeq$$

$$\simeq \left[1 + \frac{(\gamma - 1)}{2} \frac{1}{(\gamma\epsilon_I)^{1/2}} \frac{\kappa}{(1 - \kappa)}\right]\epsilon_I^{1/2}\left(\frac{\dot{M}_j V_j^\circ}{\pi P_0}\right)^{1/2} \quad , \tag{22}$$

and

$$2bR_0 \simeq \frac{\phi^2}{2\alpha}\epsilon_I^{1/2}\left(\frac{\dot{M}_j V_j^\circ}{\pi P_0}\right)^{1/2} \simeq$$

$$\simeq \frac{(1 - \kappa)}{(\gamma - 1)}\left[1 + \frac{(\gamma - 1)}{2} \frac{1}{(\gamma\epsilon_I)^{1/2}} \frac{\kappa}{(1 - \kappa)}\right]^2 \frac{\epsilon_I^{1/2}}{M_j^\circ}$$

$$\left(\frac{\dot{M}_j V_j^\circ}{\pi P_0}\right)^{1/2} \quad . \tag{23}$$

It is interesting to estimate the strength of the shock close to the point where it meets the axis. First we see from equation (15) that the shock makes an angle ϕ to the axis at this point ($\theta \cong 0$). Then, assuming that the free-expanding material within the jet moves nearly parallel to the axis for small θ, the shock velocity of the incident shock at the first crossing-shock is

$$V_{SI} \cong V_j^\circ \sin\phi \quad ; \tag{24}$$

which, for highly supersonic jets (using equations (4) and (17)), reduces to

$$V_{SI} \cong \frac{2(1-\kappa)}{(\gamma-1)}\left[1+\frac{(\gamma-1)}{2}\frac{1}{(\gamma\epsilon_I)^{1/2}}\frac{\kappa}{(1-\kappa)}\right]c_j^\circ \ . \qquad (25)$$

Equation (25) implies that the shock velocity of the incident shock (which measures the strength of the shock) is independent of the jet's velocity or its mass loss rate and depends rather weakly, on the ratio (P_0/P_j°). It is mainly determined by the sound speed (or temperature) of the jet at *injection*. This result and its implications will be discussed below.

To complete the description of the incident shock near the point it meets the axis let us estimate its pre-shock density and the properties of the flow behind it. For this purpose we refer to Figure 2. The pre-incident-shock density, can be obtained from equation (9), vis.,

$$\rho_I^\circ = \frac{P_0}{\epsilon_I V_{SI}^2} \ , \qquad (26)$$

with V_{SI} given by equation (24) (or approximately by equation (25)). If ρ_1 and V_1 are the density and velocity of the flow just behind the shock (see Figure 2), and β is the angle between V_1 and the shock, it can be shown that

$$V_1 = V_j^\circ \frac{\cos\phi}{\cos\beta} \ , \qquad (27)$$

with

$$tg\beta = \xi_I \, tg\phi \qquad (28)$$

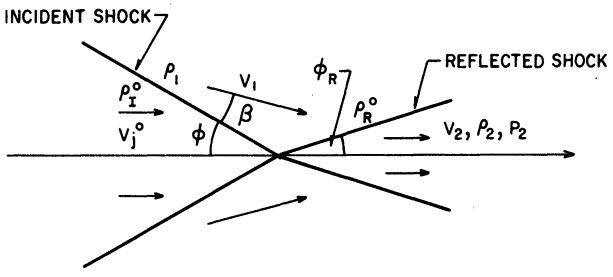

Fig. 2. A scheme showing the flow parameters close to the point where the crossing-shock intersects the axis. The incident flow moves nearly parallel to the axis and has density ρ_I° and velocity V_j°. Behind the incident shock the density is ρ_1 and the velocity V_1. As the flow moves towards the axis, the density increases up to a value ρ_R° just in front of the reflected shock. The flow leaves this later shock moving parallel to the axis, with density ρ_2, velocity V_2 and pressure P_2 greater than the ambient pressure.

and

$$\rho_1 = \frac{1}{\xi_I}\rho_I^\circ \ ; \qquad (29)$$

where ξ_I is the inverse of the compression factor across the shock. For a strong adiabatic shock

$$\xi_I = \frac{(\gamma-1)}{(\gamma+1)} \ , \qquad (30)$$

while for a strong radiative shock

$$\xi_I = \frac{2\omega}{1+(1-4\omega)^{1/2}} \ ; \qquad (31)$$

where

$$\omega \equiv \frac{1}{\gamma}\left[\frac{c}{V_{SI}}\right]^2$$

and c is the adiabatic sound speed at the equilibrium temperature behind the shock ($\cong 10^4$ °K).

As mentioned before, the basic role of the incident shock is to recollimate the free-expanding flow within the jet, turning it towards the axis. A conical converging flow is thus formed behind the incident shock. As this conical flow narrows down, a standing conical shock (the reflected shock) forms with its vertex placed at the point where the incident shock meets the axis. The flow is refracted across this shock and a narrow cylindrical stream or jet of shocked material moving along the axis is formed. It will be shown below that the pressure of this newly formed jet, coming out from the reflected shock, is much higher (by a factor of $\sim$ 20) than that of the surroundings. Thus, it will expand again trying to match its pressure with that of the ambient medium giving rise to a new incident-reflected shock pair, and so on. In this manner a series of standing crossing-shock patterns is expected to be formed within the jet.

Let us know estimate the parameters of the reflected shock. Near the jet's axis, the reflected shock can be approximated as conical, with an opening angle, ϕ_R, determined by the condition that the flow behind the shock moves parallel to the axis (see Figure 2). The problem at hand is nearly identical to that studied by Cantó, Tenorio-Tagle and Rozyczka (1988) in the context of the convergence of supersonic conical flows. We refer the reader to this paper for further details. Let ξ_R be the inverse of the compression factor across the shock, then the opening angle ϕ_R is determined by

$$tg\,\phi_R = \xi_R \, tg\,(\phi + \phi_R - \beta) \ , \qquad (32)$$

where we have used the fact that the flow converges towards the axis with an angle of incidence $\varphi - \beta$. The velocity V_2 of the stream coming out from the reflected shock is

$$V_2 = V_1 \frac{\cos(\phi + \phi_R - \beta)}{\cos\phi_R} \quad , \tag{33}$$

while its density and pressure are

$$\rho_2 = \frac{1}{\xi_R}\rho_R^\circ \tag{34}$$

and

$$P_2 = \epsilon_R \rho_R^\circ V_{SR}^2 \quad , \tag{35}$$

respectively. Where ϵ_R is a factor of order unity (see equation (8)), ξ_R is the inverse of the compression factor across the shock,

$$V_{SR} = V_1 \sin(\phi + \phi_R - \beta) \tag{36}$$

is the shock velocity, and ρ_R° is the pre-reflected-shock density given approximately by

$$\rho_R^\circ \simeq \rho_1 \left[1 + \frac{tg(\phi - \beta_R)}{tg\,\phi_R}\right] \quad . \tag{37}$$

The factor in brackets accounts for the increase in density due to the convergence of the stream towards the axis.

b) *Adiabatic Crossing-Shocks*

In order to get some insight into the results and properties of the model just described, let us consider a highly supersonic jet and assume that both, the incident and the reflected shocks are strong and adiabatic (that is, $\epsilon_I = \epsilon_R = 2/(\gamma + 1)$ and that $\xi_I = \xi_R = (\gamma - 1)/(\gamma + 1)$).

For $\gamma = 5/3$ and a helium to hydrogen particle ratio of 0.1, equation (25) yields

$$\left[\frac{V_{SI}}{km\ s^{-1}}\right] \cong 31.2(1 - 0.7\kappa)\left(1 + \frac{\chi}{1.1}\right)^{1/2}\left(\frac{T_j^\circ}{10^4\ ^\circ K}\right)^{1/2} \quad , \tag{38}$$

where χ is the hydrogen fractional ionization (helium is assumed neutral), and T_j° is the jet's temperature at injection. For $T_j^\circ = 10^4$ °K, and nearly neutral flows ($\chi << 1$), V_{SI} is expected to be in the range 9.4 km s^{-1} ($P_0/P_j^\circ \lesssim 1$) to 31.2 km s^{-1} ($P_0/P_j^\circ << 1$). The effect of considering fully-ionized-hydrogen flows ($\chi \cong 1$) is to shift the velocity range to 13 – 43.1 km s^{-1}.

The position of the crossing-shock (that is, its distance to the injection point) is given by equation (22). If n_0 and ΔV_0 are the density and velocity dispersion of the ambient medium, then $P_0 = n_0 m_0 \Delta V_0^2$ ($m_0 \sim 2m_H$ the average mass per particle) and equation (22) can be expressed as

$$\left[\frac{aR_0}{10^{17}cm}\right] = 2.13\left[1 + 0.3\frac{\kappa}{(1-\kappa)}\right]\times$$

$$\times\left[\frac{\dot{M}_j}{10^{-8}\ M_\odot\ yr^{-1}}\right]^{1/2}\left[\frac{V_j^\circ}{100\ km\ s^{-1}}\right]^{1/2}\times$$

$$\times\left[\frac{n_0}{10^3\ cm^{-3}}\right]^{-1/2}\left[\frac{\Delta V_0}{km\ s^{-1}}\right]^{-1} \quad . \tag{39}$$

The particle density entering the incident shock follows from equations (26) and (38),

$$\left[\frac{n_I^\circ}{cm^{-3}}\right] \cong 1.9\, n_0\left[\frac{\Delta V_0}{V_{SI}}\right]^2 \cong 2.0\left[\frac{n_0}{10^3\ cm^{-3}}\right]\times$$

$$\times\left[1 - 0.7\kappa\right]^{-2}\left[1 + \frac{\chi}{1.1}\right]^{-1}\left[\frac{T_j^\circ}{10^4\ ^\circ K}\right]^{-1}\left[\frac{\Delta V_0}{km\ s^{-1}}\right]^2 \quad . \tag{40}$$

The parameters of the flow behind the incident shock are,

$$n_1 = 4n_I^\circ \quad , \quad \beta \cong \phi/4 \quad , \quad V_1 \cong V_j^\circ \quad . \tag{41}$$

Regarding the reflected shock, we first notice that, if $\xi_I = \xi_R$ equations (28) and (32) imply

$$\phi_R = \beta \cong \frac{\phi}{4} \quad , \tag{42}$$

and thus equation (36) reduces to

$$V_{SR} \cong V_1 \sin\phi \cong V_j^\circ \sin\phi \cong V_{SI} \quad . \tag{43}$$

That is, the shock velocity of the reflected shock is approximately equal to the shock velocity of the incident shock. Therefore, the entire crossing-shock is characterized by a single shock velocity, given by equation (38) which is in the range 9.4 – 43.1 km s^{-1}.

The particle density, n_R°, entering the reflected shock follows from equation (37)

$$n_R^\circ \cong n_1\left[1+\frac{(\phi-\beta)}{\phi_R}\right] \quad . \tag{44}$$

Substitution of equations (41) and (42) in equation (44) yields

$$n_R^\circ = 16\, n_j^\circ \quad , \tag{45}$$

with n_1° given by equation (40)

Assuming that the surface brightness (F) of a shock is proportional to the pre-shock density, from equation (44) it follows that the reflected shock will dominate the emission of the crossing-shock by a factor

$$\frac{F(reflected)}{F(incident)} \sim \frac{n_R^\circ}{n_j^\circ} \sim 16 \quad , \tag{46}$$

since the shock velocities for both shocks are expected to be very similar (equation (43)).

The density and, most important, the pressure of the stream coming out from the reflected shock, can be found from equations (34) and (35). They are

$$n_2 = 64\, n_j^\circ \quad , \tag{47}$$

and

$$P_2 \cong 16\, P_0 \quad , \tag{48}$$

where we have used equations (26), (43) and (45).

This outflowing highly collimated supersonic stream represents a new overpressured jet injected into the surroundings. It will expand producing another incident-reflected shock pair or crossing-shock. We can thus apply the equations described above to find the properties of the next crossing-shock.

If the shock velocity of the first crossing-shock is in the range 9.4 – 43.1 km s^{-1}, the shock models of Shull and McKee (1979) indicate a rather small fractional ionization behind the shock. Thus we can set $\chi \cong 0$ in equation (38). Furthermore, since the pressure ratio $(P_0/P_j^\circ) \cong 1/16$ according to equation (48), the parameters of the second crossing-shock will be

$$\left[\frac{V_{SI}}{km\ s^{-1}}\right] \cong \left[\frac{V_{SR}}{km\ s^{-1}}\right] \cong 18.7\left[\frac{T_j^\circ}{10^4\ ^\circ K}\right]^{1/2} \quad , \tag{49}$$

$$\left[\frac{aR_0}{10^{17}\ cm}\right] \cong 3.0\left[\frac{\dot{M}_j}{10^{-8}\ M_\odot\ yr^{-1}}\right]^{1/2} \times$$

$$\times\left[\frac{V_j^\circ}{100\ km\ s^{-1}}\right]^{1/2}\left[\frac{n_0}{10^3\ cm^{-3}}\right]^{-1/2}\times\left[\frac{\Delta V_0}{km\ s^{-1}}\right]^{-1} \quad , \tag{50}$$

$$\left[\frac{n_j^\circ}{cm^{-3}}\right] \cong 5.4\left[\frac{n_0}{10^3\ cm^{-3}}\right]\left[\frac{T_j^\circ}{10^4\ ^\circ K}\right]^{-1}\left[\frac{\Delta V_0}{km\ s^{-1}}\right]^2 \quad , \tag{51}$$

with n_R° and the density and pressure of the new jet given by equations (44), (47) and (48).

Clearly, in equations (49) and (51), T_j° now represents the temperature of the jet that emerges from the previous crossing-shock. Since this temperature is proportional to the square of the shock velocity (for adiabatic shocks) this will necessarily lead to an unstable situation in the sense that the shock velocity for successive crossing-shocks will rapidly increase destroying the jet after only a few shocks. Indeed, considering a jet with an initial temperature of 10^4 °K, the first crossing-shock will have a shock velocity of $\sim$ 18.7 km s^{-1} according to equation (49). For a strictly adiabatic shock, the temperature of the emergent jet will be $\sim$ 15 200 °K. Thus, the shock velocity for the next crossing-shock will be $\sim$ 35 km s^{-1}, which will lead to a jet with a temperature of $\sim$ 35 000 °K, etc.

We must note, however, that such an unstable situation is a direct consequence of the assumption that the shocks are adiabatic. This assumption is not valid for shock velocities $\geqslant$ 20 km s^{-1} according to Cantó, Tenorio-Tagle and Rozyczka (1988) (their Appendix B). They find that reflected shocks (their conical collimating shocks) with shock velocities between $\sim$ 20 to 200 km s^{-1} are best approximated as radiative with an equilibrium temperature $\sim 10^4$ °K, and thus the instability described above is inhibited. In the next section radiative crossing-shocks will be considered.

c) *Radiative Crossing-Shocks*

In this section, we will assume that both, the incident and the reflected shocks are radiative with a post-shock equilibrium temperature of 10^4 °K. For a highly supersonic jet with $\gamma = 5/3$ and a 0.1 helium to hydrogen particle density ratio, equation (25) reduces to

$$\left[\frac{V_{SI}}{km\ s^{-1}}\right] \cong 31.2\left[1-\left(1-\frac{0.26}{\epsilon_I^{1/2}}\right)\kappa\right] \quad , \tag{52}$$

where we have assumed $\chi << 1$ since we expect shock velocities $\leqslant$ 40 km s^{-1} (see above). In equation (52) the parameter $\epsilon_I \cong 1$ and can be expressed as

$$\epsilon_I = 1 - \xi_I \quad , \tag{53}$$

with ξ_I given by equation (31).

In the limit of small ϕ, β and ϕ_R (highly supersonic jets), equations (27), (28), (32) and (33) reduce to

$$\beta \cong \xi_I \phi \quad , \tag{54}$$

$$V_1 \cong V_j^\circ \quad , \tag{55}$$

$$\phi_R \cong \frac{\xi_R(1-\xi_I)}{(1-\xi_R)}\phi \quad , \tag{56}$$

$$V_2 \cong V_j^\circ \quad ; \tag{57}$$

and thus, equations (35), (36) and (37) can be written as

$$V_{SR} \cong \frac{(1-\xi_I)}{(1-\xi_R)} V_{SI} \quad , \tag{58}$$

$$P_2 \cong \frac{(1-\xi_I)}{(1-\xi_R)} \frac{1}{\xi_I \xi_R} P_0 \quad , \tag{59}$$

$$\rho_R^\circ \cong \frac{1}{\xi_R}\rho_1 \quad , \tag{60}$$

with ρ_I°, ρ_1 and ρ_2 given by equations (26), (29) and (34) respectively. In the above equations we have used

$$\epsilon_R = 1 - \xi_R \quad , \tag{61}$$

where ξ_R is given by an expression similar to equation (31) (with $V_{SI} = V_{SR}$).

As in §II.b, P_2 in equation (59) represents the pressure of the outcoming supersonic stream, which will produce the next crossing-shock. Thus, we can substitute P_0/P_2 from equation (59) instead of P_0/P_j° in equation (52) in order to obtain self-consistency. First, we notice the symmetry of equation (58) with respect to an interchange between V_{SI} and V_{SR} (ξ_I and ξ_R depend on V_{SI} and V_{SR}, respectively, in the same way; see equation (31)). Thus

$$V_{SR} \cong V_{SI} \quad . \tag{62}$$

That is, we reach the same conclusion as in the case of adiabatic shocks: the entire crossing-shock is characterized by a *single* shock velocity, that given by equation (52). Using equation (62), $\xi_R \cong \xi_I$ and substituting equations (59) and (53) in equation (52) one obtains

$$\left[\frac{V_{SI}}{km\ s^{-1}}\right] \cong 31.2 \times \left\{1 - \left[1 - \frac{0.26}{(1-\xi_I)^{1/2}}\right]\xi_I^{0.4}\right\} \quad , \tag{63}$$

with ξ_I given by equation (31). The solution of equations (31) and (63) is

$$V_{SI} \cong 18.7\ km\ s^{-1} \quad . \tag{64}$$

Therefore, we reach the important conclusion that radiative crossing-shocks within overpressured highly supersonic jets will *always* be characterized by a shock velocity of ~ 18.7 km s^{-1} quite independent of either the parameters of the jet or those of the ambient medium.

Using equation (64) we can find the other parameters of the model, the compression factors accross the shocks

$$\xi_I \cong \xi_R \cong 0.245 \quad , \tag{65}$$

the pressure of the jet emerging from each crossing-shock

$$P_2 \cong 16.7\ P_0 \quad ; \tag{66}$$

the distance between crossing-shocks (from equation (39))

$$\left[\frac{aR_0}{10^{17}\ cm}\right] \cong 3.0\left[\frac{\dot{M}_j}{10^{-8}\ M_\odot\ yr^{-1}}\right]^{1/2}\left[\frac{V_j^\circ}{100\ km\ s^{-1}}\right]^{1/2} \times$$

$$\times\left[\frac{n_0}{10^3\ cm^{-3}}\right]^{-1/2}\left[\frac{\Delta V_0}{km\ s^{-1}}\right]^{-1} \quad , \tag{67}$$

the pre-incident-shock particle density (from equation (26))

$$\left[\frac{n_I^\circ}{cm^{-3}}\right] \cong 5.4\left(\frac{n_0}{10^3\ cm^{-3}}\right)\left[\frac{\Delta V_0}{km\ s^{-1}}\right]^2 \quad , \tag{68}$$

the particle density behind the incident shock (from equation (29))

$$n_1 = 4.1\ n_I^\circ \quad , \tag{69}$$

the pre-reflected-shock particle density (from equation (60))

$$n_R^\circ = 16.7\ n_I^\circ \quad , \tag{70}$$

and the particle density in the emerging jet

$$n_2 \cong 68.33\, n_j^\circ \quad . \tag{71}$$

From equation (70) we see that the reflected shock will dominate the emission of the crossing-shock by a factor of $\sim$ 16.7. In order to compare our model with the observations we have to estimate the electron density behind the reflected shock. Shull and McKee (1979) have studied shocks with velocities in the range 40 – 130 km s^{-1}. From their results we estimate that the post-shock hydrogen ionization fraction scales as $\sim V_S^{3.5}$ for V_S between 40 – 60 km s^{-1}. Extrapolating to lower velocities we found a fractional ionization of $\sim 10^{-2}$ for $V_S \sim 20$ km s^{-1}. Thus, the electron density behind the reflected shock will be

$$n_e \sim 0.68\, n_j^\circ \quad , \tag{72}$$

or from equation (68)

$$\left[\frac{n_e}{cm^{-3}}\right] \sim 3.7\left[\frac{n_0}{10^3\, cm^{-3}}\right]\left[\frac{\Delta V_0}{km\ s^{-1}}\right]^2 \quad . \tag{73}$$

Equation (73) shows another important result of our model, that is that the electron density in the crossing-shocks depends *only* on the parameters (density and velocity dispersion; that is on the pressure) of the ambient medium, and not on the parameters of the jet itself.

The other parameters of interest, such as the opening angle of the free-expanding part of the jet

$$\alpha_1(^\circ) \cong 7.7\left[\frac{V_j^\circ}{100\ km\ s^{-1}}\right]^{-1} \quad , \tag{74}$$

its length (in units of the separation between crossing-shocks)

$$\frac{R_*}{aR_0} = \left[1 - \frac{\alpha}{\phi}\right] = 0.28 \quad , \tag{75}$$

the angle between the incident shock and the axis of the jet

$$\phi(^\circ) \cong 10.7\left[\frac{V_j^\circ}{100\ km\ s^{-1}}\right]^{-1} \quad , \tag{76}$$

and the opening angle of the reflected shock

$$\phi_R(^\circ) \cong 2.6\left[\frac{V_j^\circ}{100\ km\ s^{-1}}\right]^{-1} \quad , \tag{77}$$

follow from equations (4), (A.1), (17), and (56).

III. CONCLUSIONS

We present the results of an analytic study of the internal structure of steady jets running into a uniform medium. The model is restricted to underexpanded highly supersonic narrow jets. In this case, the jet develops internal crossing-shock as it tries to match its pressure with that of the ambient medium.

The model gives simple analytic expressions for the main parameters of the crossing-shocks such as their shapes, the distance between them, the pre-shock density, and the shock velocity (that is the velocity which determines the excitation).

Our main conclusions are the following: 1) the locus of the incident shock (that is, the locus of the intersection of this shock, which is a surface, with a plane containing the symmetry axis) is an arc of circumference passing through the injection point. 2) The distance between consecutive crossing-shocks is given by

$$(aR_0) = \lambda\left(\frac{\dot{M}_j V_j^\circ}{\pi P_0}\right)^{1/2} \quad ,$$

where $\dot{M}_j$ is the mass loss rate in the jet, V_j° its velocity at injection, P_0 is the external medium pressure, and λ is a parameter of order unity which depends (rather weakly) on the ratio between the initial thermal pressure of the jet and P_0. It is found that regardless of the initial conditions the jet enters into a self-regulated state in which this ratio is $\sim 1/17$, and $\lambda \gtrsim 1.2$. 3) For highly supersonic jets, the velocity of the jet changes only slightly across the shocks (they are very oblique) and thus jets running into a uniform medium develop nearly equidistant crossing-shocks. 4) For radiative crossing-shocks with equilibrium temperature $\sim 10^4$ °K, the shocks will *always* be characterized by a shock velocity of ~ 20 km s^{-1}, quite independent of either the parameters of the jet or those of the ambient medium. 5) The electron density in the crossing-shocks depends *only* on the pressure of the ambient medium and not on the parameters of the jet itself.

In subsequent papers we will present a more complete description of the dynamical structure and observational characteristics of the crossing-shocks through a detailed numerical study of the problem. In particular, we will inquire on the basic premises of the present simplified model, and on the approximations we had to make in order to solve the problem by analytic methods.

REFERENCES

Bührke, T., Mundt, R., and Ray, T.P. 1988, *Astr. and Ap.*, **200**, 99.
Blandford, R.D. and Rees, M.J. 1974, *M.N.R.A.S.*, **169**, 395.
Blondin, J.M., Königl, A., and Fryxell, B.A. 1989, in press.
Cantó, J. 1980, *Astr. and Ap.*, **86**, 327.
Cantó, J., Sarmiento, A., and Rodríguez, L.F. 1986, *Rev. Mexicana Astron. Astrof.*, **13** 107.
Cantó, J., Tenorio-Tagle, G., and Rozyczka, M. 1988, *Astr. and Ap.*, **192**, 287.
Cohn, H. 1983, *Ap. J.*, **269**, 500.
Crighton, D.G. 1981, *J. Fluid Mech.*, **106**, 261.
Falle, S.A.E.G. and Wilson, M.J. 1985, *M.N.R.A.S.*, **216**, 79.
Falle, S.A.E.G., Innes, D.E., and Wilson, M.J. 1987, *M.N.R.A.S.*, **225**, 741.
Ferrari, A., Trussoni, E., and Zaninetti, L. 1981, *M.N.R.A.S.*, **196**, 1051.
Mundt, R. 1986, *Canadian J. of Phys.*, **64**, 407.
Mundt, R. 1988, in *NATO ASI, Formation and Evolution of Low Mass Stars*, eds. A.K. Dupree and M.T.V.T. Lago, p. 150.
Norman, M.L., Smarr, L., Winkler, K.-H.A., and Smith, M. D. 1982, *Astr. and Ap.*, **113**, 285.
Payne, D.G. and Cohn, H. 1985, *Ap. J.*, **291**, 665.
Prandtl, L. 1907, *Phys. Zs.*, **8**, 23.
Raga, A.C. and Mateo, M. 1988, *A.J.*, **95**, 543.
Raga, A.C. 1989, *Ap. J.*, in press.
Reipurth, B., Bally, J., Graham, J.A., Lane, A.P., and Zealey, W.J. 1986, *Astr. and Ap.*, **164**, 51.
Sanders, R.H. 1983, *Ap. J.*, **266**, 73.
Shull, J.M. and McKee, C.F. 1979, *Ap. J.*, **227**, 131.
Silvestro, G., Ferrari, A., Rosner, R., Trussoni, E., and Tsinganos, K. 1987, *Nature*, **325**, 228.
Tenorio-Tagle, G., Rozyczka, M., and Cantó, J. 1986, in *Workshop on Model Nebulae*, ed. D. Pequignot (Paris: Publication de l'observatoire de Paris), p. 263.
Tenorio-Tagle, G. and Rozyczka, M. 1988, private communication.
Wilson, M.J. and Falle, S.A.E.G. 1985, *M.N.R.A.S.*, **216**, 971.
Wilson, M.J. 1987*a*, *M.N.R.A.S.*, **224**, 155.
Wilson, M.J. 1987*b*, *M.N.R.A.S.*, **226**, 447.

APPENDIX

Consider the minus sign in equation (15), corresponding to the $y > 0$ arc. Let r_* be the radius at intersection (in units of R_0). Then,

$$r_* = \sin(\phi - \alpha) \quad . \tag{A. 1}$$

The pressure in the jet can be expressed as

$$P_j = \frac{1}{\gamma} \rho_j c_j^2 \quad . \tag{A. 2}$$

In particular,

$$P_j^\circ = \frac{1}{\gamma} \rho_j^\circ c_j^{\circ\,2} \quad , \tag{A. 3}$$

where ρ_j° is the jet's density at injection.

For an adiabatic expansion

$$\frac{P_j}{P_j^\circ} = \left[\frac{\rho_j}{\rho_j^\circ}\right]^\gamma \quad , \tag{A. 4}$$

which, after substitution of equation (A.3), can be written as

$$\frac{P_j}{P_j^\circ} = \left[\frac{c_j^{\circ\,2}}{\gamma P_j^\circ} \rho_j\right]^\gamma \quad . \tag{A. 5}$$

From equation (5), and introducing the definitions of R_0 (equation (12)) and r (equation (13)), the jet's density can be expressed as

$$\rho_j(r) = \left[\frac{P_0}{\epsilon_I V_j^{\circ 2}}\right] \frac{1}{r^2} \quad . \tag{A. 6}$$

Substituting equation (A.6) in equation (A.5) one obtains

$$\frac{P_j}{P_j^\circ} = \left[\left(\frac{1}{\gamma\epsilon_I}\right) \frac{1}{M_j^{\circ 2}} \left(\frac{P_0}{P_j^\circ}\right)\right]^\gamma \frac{1}{r^{2\gamma}} \tag{A. 7}$$

which gives the pressure of the jet as a function of distance from the injection point. For $r = r_*$, $P_j = P_0$ and equation (A.7) yields

$$r_* = \left[\frac{1}{\gamma\epsilon_I}\right]^{1/2} \frac{1}{M_j^\circ} \left[\frac{P_0}{P_j^\circ}\right]^{(\gamma-1)/2\gamma} \quad , \tag{A. 8}$$

and from equation (A.1)

$$\phi = \alpha + \arcsin\left[\left(\frac{1}{\gamma\epsilon_I}\right)^{1/2} \left(\frac{1}{M_j^\circ}\right) \left(\frac{P_0}{P_j^\circ}\right)^{(\gamma-1)/2\gamma}\right] \quad . \tag{A. 9}$$

Jorge Cantó: Instituto de Astronomía, UNAM, Apartado Postal 70-264, 04510 México, D.F., México.
Luc Binette and Alejandro C. Raga: Canadian Institute for Theoretical Astrophysics, University of Toronto, 60 St. George Street, Toronto, Ontario M5S 1A1, Canada.